Testing for Markovian Character and Modeling of Intermittency in Solar Wind Turbulence

Marek Strumik*

Space Research Centre, Polish Academy of Sciences, Bartycka 18 A, 00-716 Warsaw, Poland

Wiesław M. Macek

Faculty of Mathematics and Natural Sciences. College of Sciences, Cardinal Stefan Wyszyński University, Dewajtis 5, 01-815 Warsaw; Space Research Centre, Polish Academy of Sciences, Bartycka 18 A, 00-716 Warsaw, Poland

(Dated: February 2, 2008)

Abstract

We present results of statistical analysis of solar wind turbulence using an approach based on the theory of Markov processes. It is shown that the Chapman-Kolmogorov equation is approximately satisfied for the turbulent cascade. We evaluate the first two Kramers-Moyal coefficients from experimental data and show that the solution of the resulting Fokker-Planck equation agrees well with experimental probability distributions. Our results suggest the presence of a local transfer mechanism for magnetic field fluctuations in solar wind turbulence.

PACS numbers: 96.50.Tf,02.50.Ga,02.50.Fz,05.10.Gg

*Electronic address: maro@cbk.waw.pl

I. INTRODUCTION

Irregular dynamics of the solar wind plasma exhibits many similarities to fully developed hydrodynamic turbulence. Numerous in situ measurements of temporal variability of parameters of the plasma have shown that their spectral distributions usually have power-law character [1, 2, 3, 4]. Investigations of the fluctuations have also revealed their non-Gaussian probability distributions at small scales, which is commonly attributed to intermittency phenomenon [5, 6, 7, 8]. In fact, the solar wind provides a unique laboratory for studying high-Reynolds-number magnetohydrodynamic turbulence (see, e.g., Refs. [2, 9] for review).

One of the main problems in the studies of incompressible hydrodynamical turbulence is explaining the statistics of velocity fluctuations on different length scales. In magnetohydrodynamic turbulence this problem concerns in general also magnetic field and density fluctuations. Conventionally, in investigations of a turbulent cascade, statistical properties of fluctuations $\delta u_\tau(t) = u(t+\tau) - u(t)$ of a physical quantity $u(t)$ are examined, where τ is temporal (or spatial) scale. The fluctuations are studied by examining their probability distribution functions (p.d.f.) $P(\delta u_\tau(t))$ or n-order moments $\langle \delta u_\tau(t)^n \rangle$ of the distributions, called also structure functions. Often, if the root-mean-square of velocity fluctuations is small as compared to the mean velocity of the flow, one can use the Taylor hypothesis, interpreting the temporal variation δu_τ at a fixed position as a spatial variation δu_l, where l is a spatial scale corresponding to the temporal scale τ. In an intermittent turbulent cascade, the p.d.f. of the fluctuations is non-Gaussian at small scales. When we go to larger scales, the shape of the p.d.f. changes, and finally there is a scale τ_G, such that for $\tau > \tau_G$ the p.d.f. is close to Gaussian distribution [10, 11].

A number of models for the scaling exponents and scaling of the probability distributions of the fluctuations have been proposed. Many papers have been also devoted to experimental verification of the proposed models (see, e.g., Refs. [9, 10, 11] for review). Recently, a great deal of attention has been devoted to investigations of the fluctuations in hydrodynamic turbulence from the point of view of the Markov processes theory (see, e.g., Refs. [12, 13, 14, 15, 16, 17]). In particular, results of the verification of the validity of the Chapman-Kolmogorov equation as well as estimations of the Kramers-Moyal coefficients from experimental data suggest that the Markov processes approach may be appropriate to the description and modeling of the turbulent cascade [13, 14, 17]. The estimations of the

Kramers-Moyal coefficients allow to determine the form of the Fokker-Planck equation governing the evolution of the probability distribution with scale for the fluctuations. A model based on a Fokker-Planck equation has been recently proposed for solar wind turbulence, but for fluctuations of quantities that exhibit self-similar scaling [18]. In the present paper, the Markov processes approach for the first time has been applied to analysis of intermittent solar wind turbulence. This approach seems to provide a contact point between pure statistics and dynamical systems approach to turbulence.

II. DATA SET

In the plasma flow expanding from the Sun into the interplanetary space we can distinguish several forms, in particular the slow ($<$ 450 km/s) and fast ($>$ 600 km/s) solar wind (see, e.g., Ref. [19] and references therein). At the solar minimum the two forms are usually well separated, the fast wind is more homogeneous and incompressible in comparison with the slow wind. Our goal here is to study properties of the turbulent cascade, therefore we try to exclude effects associated with nonstationary driving and spatial inhomogeneity of the turbulence. For this reason, in this paper we have chosen for analysis the fast solar wind flowing from non-active high-latitude regions in the solar corona at the solar minimum. This data set represents dynamics of fast solar wind free of dynamical interaction with slow wind, as possibly the most homogeneous and probably also most stationary case. Therefore effects associated with nonstationary driving should be eliminated here to a large extent, and we should observe a state possibly closest to freely decaying turbulence, which seems to be the most appropriate case to study the turbulent cascade. Since we would like to examine fluctuations in a wide range of scales, including small scales, we focus here on magnetic field fluctuations, which are available at much better time resolution in comparison with measurements of plasma parameters (e.g., bulk velocity or density of the plasma). However, we are aware of the importance of detailed analysis of other types of the solar wind, as well as other bulk plasma parameters, and we are going to carry out such studies in a future.

The data set analyzed here consists of about 1.3×10^7 measurements of the radial component B_R of the magnetic field obtained by the Ulysses spacecraft from 70:1996 to 230:1996 (day of year:year) at time resolution of one second (see Ref. [20] for the description of the experimental setup). The measurements have been obtained at heliospheric latitudes from

29 to 44 degree and at radial distance from the Sun from 3.5 to 4.2 AU. Small gaps (up to three missing points) in the data set have been filled using linear interpolation. Further in this paper we consider fluctuations of the radial component of the magnetic field defined as $b_\tau(t) = B_R(t+\tau) - B_R(t)$. Presenting results of our analysis, we do not recast the fluctuations into the space domain via the Taylor hypothesis, i.e., we consistently use here temporal scales. However, since we analyze highly supersonic and super-Alfvénic flow (mean velocity $U \approx 744$ km/s in the reference system moving with the measuring instrument), the temporal scales physically should be interpreted rather as spatial scales. Assuming that the Taylor hypothesis is satisfied here, one can easily transform the temporal scale τ to the spatial scale l using the relationship $l = U\tau$ [10]. However, since Ulysses spacecraft provides one-point measurements of the magnetic field, in general it is not possible to distinguish between temporal and spatial variations in this case.

In Fig. 1 we show the power spectrum of the radial component of the magnetic field.

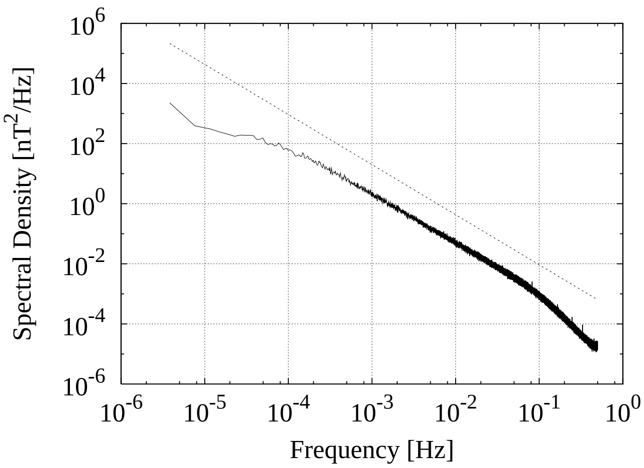

FIG. 1: Power spectrum of the radial component of the solar wind magnetic field (solid line). The dashed line shows the spectrum of the type $E(f) \propto f^{-5/3}$ for comparison.

As one can see, the power spectrum has a power-law character with spectral exponent very close to -5/3 in the inertial range identified here as stretching approximately from 0.0002 to 0.075 Hz.

III. MARKOV PROCESSES APPROACH

In the case of a Markov process, by definition the following condition must be satisfied

$$P(b_{\tau_1}, \tau_1 | b_{\tau_2}, \tau_2; \ldots ; b_{\tau_N}, \tau_N) = P(b_{\tau_1}, \tau_1 | b_{\tau_2}, \tau_2), \tag{1}$$

thus the N-point joint p.d.f. $P(b_{\tau_1}, \tau_1; b_{\tau_2}, \tau_2; \ldots ; b_{\tau_N}, \tau_N)$ is determined by the product of conditional probabilities $P(b_{\tau_{i-1}}, \tau_{i-1} | b_{\tau_i}, \tau_i)$, where $\tau_{i-1} < \tau_i$. For a finite set of experimental data, the Markov property can be verified by comparison of a conditional p.d.f. $P_{\mathrm{E}}(b_{\tau_1}, \tau_1 | b_{\tau_2}, \tau_2)$ evaluated directly from data with the p.d.f. computed using the Chapman-Kolmogorov equation

$$P(b_{\tau_1}, \tau_1 | b_{\tau_2}, \tau_2) = \int_{-\infty}^{\infty} P(b_{\tau_1}, \tau_1 | b_{\tau'}, \tau') P(b_{\tau'}, \tau' | b_{\tau_2}, \tau_2) \mathrm{d}b_{\tau'}, \tag{2}$$

where $\tau_1 < \tau' < \tau_2$. Eq. (2) is a necessary condition for a stochastic process to be Markovian. The Chapman-Kolmogorov equation can be written in a differential form using the so-called Kramers-Moyal expansion

$$-\tau \frac{\partial P(b_\tau, \tau | b_{\tau_0}, \tau_0)}{\partial \tau} = \sum_{k=1}^{\infty} \left(-\frac{\partial}{\partial b_\tau} \right)^k D^{(k)}(b_\tau, \tau) P(b_\tau, \tau | b_{\tau_0}, \tau_0). \tag{3}$$

Kramers-Moyal coefficients $D^{(k)}(b_\tau, \tau)$ can be evaluated as the limit $\Delta\tau \to 0$ of the conditional moments $M^{(k)}(b_\tau, \tau, \Delta\tau)$, namely

$$D^{(k)}(b_\tau, \tau) = \lim_{\Delta\tau \to 0} M^{(k)}(b_\tau, \tau, \Delta\tau) \tag{4}$$

and

$$M^{(k)}(b_\tau, \tau, \Delta\tau) = \frac{\tau}{k!\ \Delta\tau} \int_{-\infty}^{\infty} (b_{\tau'} - b_\tau)^k P(b_{\tau'}, \tau' | b_\tau, \tau) \mathrm{d}b_{\tau'}, \tag{5}$$

where $\Delta\tau = \tau - \tau'$. If $D^{(4)}(b_\tau, \tau) = 0$ then according to the Pawula theorem: $D^{(k)}(b_\tau, \tau) = 0$ for $k \geq 3$ [21]. In this case, starting from Eq. (3) we arrive at the Fokker-Planck equation

$$-\tau \frac{\partial P(b_\tau, \tau)}{\partial \tau} = \left(-\frac{\partial D^{(1)}(b_\tau, \tau)}{\partial b_\tau} + \frac{\partial^2 D^{(2)}(b_\tau, \tau)}{\partial b_\tau^2} \right) P(b_\tau, \tau), \tag{6}$$

which determines the evolution of the probability distribution function of a stochastic process generated by the Langevin equation (Ito definition)

$$-\tau \frac{\mathrm{d}b_\tau}{\mathrm{d}\tau} = D^{(1)}(b_\tau, \tau) + \sqrt{D^{(2)}(b_\tau, \tau)}\ \Gamma(\tau), \tag{7}$$

where $\Gamma(\tau)$ is the delta-correlated Gaussian noise. In comparison with definition used in Ref. [21], the Kramers-Moyal coefficients given here are multiplied by τ, which is equivalent to a logarithmic length scale [17].

If Eq. (2) is satisfied, then the transition probability from scale τ_2 to τ_1 can be divided into transitions from τ_2 to τ' and then from τ' to τ_1. Therefore, in the case of a turbulent cascade, fulfillment of the Chapman-Kolmogorov equation for all triplets $\tau_1 < \tau' < \tau_2$ in the inertial range suggests the presence of a local transfer mechanism in the cascade.

IV. RESULTS

In Fig. 2 we show superposed contour plots of the conditional p.d.f. estimated directly

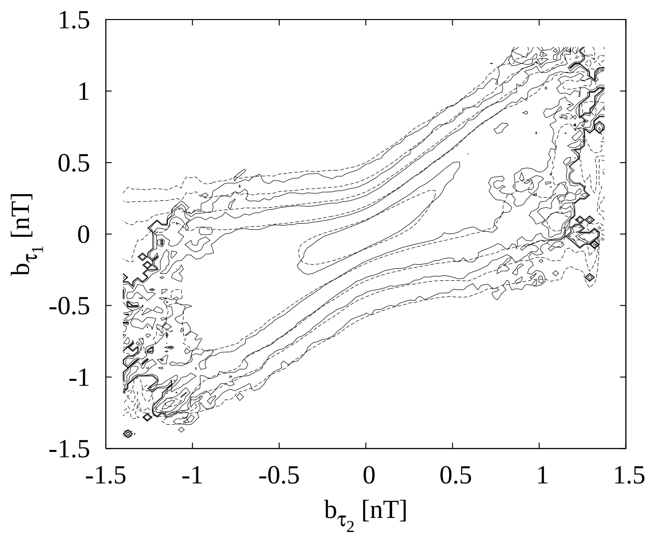

FIG. 2: Contour plots illustrating verification of the Chapman-Kolmogorov equation for $\tau_1 = 750$, $\tau' = 1000$, and $\tau_2 = 1250$ seconds. Solid lines represent the conditional p.d.f. $P_{\mathrm{E}}(b_{\tau_1}, \tau_1|b_{\tau_2}, \tau_2)$ evaluated directly from data, whereas dashed lines show the conditional p.d.f. $P(b_{\tau_1}, \tau_1|b_{\tau_2}, \tau_2)$ computed using Eq. (2). The subsequent isolines correspond to the following levels of the p.d.f.: 2.0, 0.7, 0.2, 0.07, 0.02 (from the middle of the plot).

from data and the p.d.f. computed using Eq. (2) for $\tau_1 = 750$, $\tau' = 1000$, and $\tau_2 = 1250$ seconds. One can see that corresponding contour lines for the two probability distributions are very close to each other. This indicates that the Chapman-Kolmogorov equation is (at

least approximately) satisfied for the range of scales from $\tau_1 = 750$ to $\tau_2 = 1250$ seconds. In Fig. 3 we show the cuts through the conditional probability distributions for fixed values

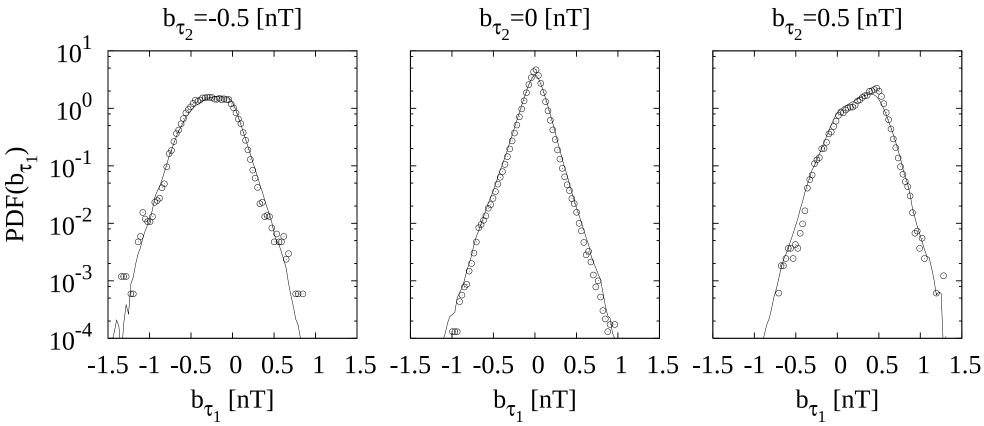

FIG. 3: Verification of the Chapman-Kolmogorov equation (2) for $\tau_1 = 750$, $\tau' = 1000$, and $\tau_2 = 1250$ seconds. Comparisons of cuts through $P_{\mathrm{E}}(b_{\tau_1}, \tau_1 | b_{\tau_2}, \tau_2)$ (points) and $P(b_{\tau_1}, \tau_1 | b_{\tau_2}, \tau_2)$ (lines) from Fig. 2 are shown for fixed values of b_{τ_2}, namely $b_{\tau_2} = -0.5$ nT (on the left), $b_{\tau_2} = 0$ nT (in the middle), and $b_{\tau_2} = 0.5$ nT (on the right).

of b_{τ_2}. As one can see, points representing cuts through $P_{\mathrm{E}}(b_{\tau_1}, \tau_1 | b_{\tau_2}, \tau_2)$ fit well to the lines representing cuts through $P(b_{\tau_1}, \tau_1 | b_{\tau_2}, \tau_2)$. Repeating such a comparison for different triplets τ_1, τ', τ_2 we have checked that Eq. (2) is well satisfied in the inertial range (for scales from about 50 to 5000 seconds). For larger scales, outside the inertial range, the larger is the scale, a worse agreement we observe between experimental p.d.f. and that computed using Eq. (2). Nevertheless, Eq. (2) seems to be fulfilled up to the scale of about 24 hours. Therefore, the necessary condition for Markov processes is satisfied here in the entire range of scales available for our computations, unlike it is in the case of hydrodynamic turbulence as reported in Ref. [17], where the cascade is not Markovian for small scales, below the Taylor length scale.

We have computed the coefficients $M^{(k)}(b_\tau, \tau, \Delta\tau)$ using the definition of Eq. (5). In Figs. 4(a) and 4(b) we present examples of the dependence of the coefficients $M^{(1)}(b_\tau, \tau, \Delta\tau)$ and $M^{(2)}(b_\tau, \tau, \Delta\tau)$ on b_τ for $\tau = 1000$ and $\Delta\tau = 100$ seconds. In Fig. 4(c) we show the dependence of $M^{(2)}(b_\tau, \tau, \Delta\tau)$ on $M^{(1)}(b_\tau, \tau, \Delta\tau)$, which have a more regular and symmetric form in comparison with the dependence of $M^{(2)}(b_\tau, \tau, \Delta\tau)$ on b_τ. We propose the

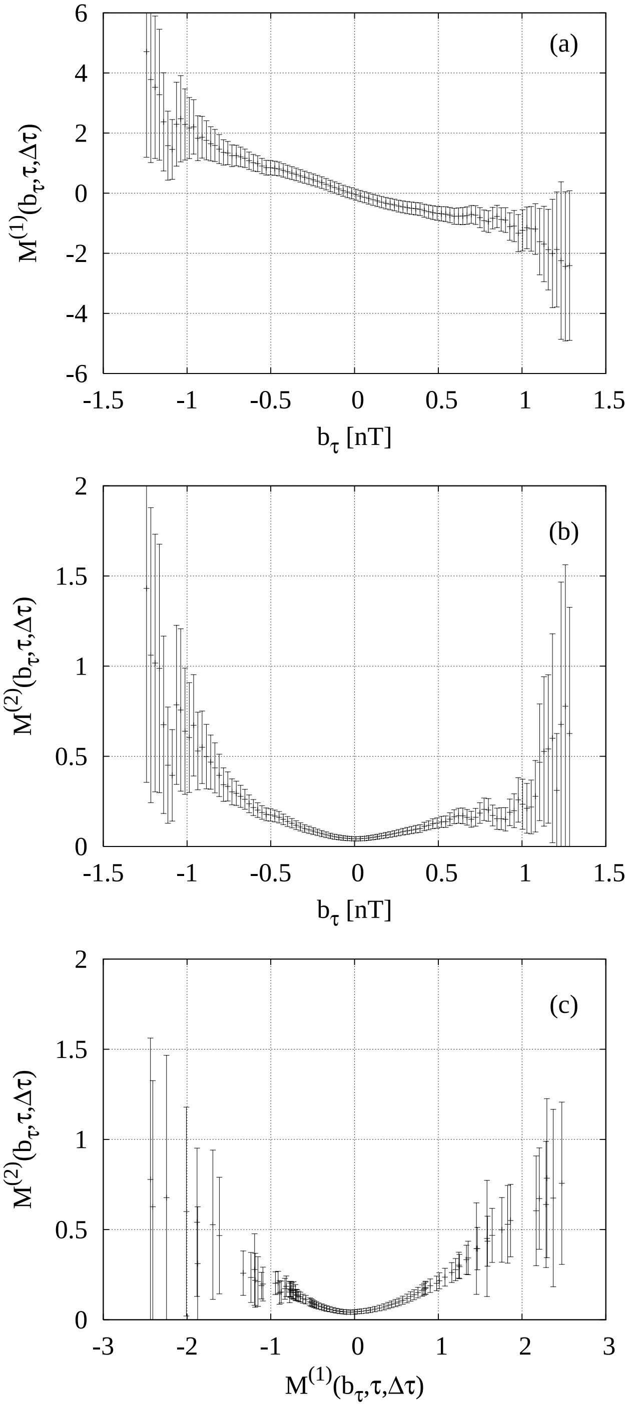

FIG. 4: The dependence of the coefficients (a) $M^{(1)}(b_\tau, \tau, \Delta\tau)$ and (b) $M^{(2)}(b_\tau, \tau, \Delta\tau)$ on b_τ for $\tau = 1000$ and $\Delta\tau = 100$ seconds. In panel (c) we show the dependence of $M^{(2)}(b_\tau, \tau, \Delta\tau)$ on $M^{(1)}(b_\tau, \tau, \Delta\tau)$.

following approximations: $M^{(1)}(b_\tau, \tau, \Delta\tau) = A_1(\tau, \Delta\tau)b_\tau + A_2(\tau, \Delta\tau)b_\tau^3 + A_3(\tau, \Delta\tau)b_\tau^5$ and

$M^{(2)}(b_\tau, \tau, \Delta\tau) = A_4(\tau, \Delta\tau) + A_5(\tau, \Delta\tau)[M^{(1)}(b_\tau, \tau, \Delta\tau)]^2$ as describing properly the experimental relationships shown in Figs. 4(a) and 4(c), correspondingly. Based on the approximations, we can fit the parameters $A_i(\tau, \Delta\tau)$ for a fixed τ and changing $\Delta\tau$, and finally compute the limits $a_i(\tau) = \lim_{\Delta\tau \to 0} A_i(\tau, \Delta\tau)$ for $i = 1 \ldots 5$ (e.g., by a linear extrapolation toward $\Delta\tau = 0$) obtaining the following approximations:

$$D^{(1)}(b_\tau, \tau) = a_1(\tau) b_\tau + a_2(\tau) b_\tau^3 + a_3(\tau) b_\tau^5 \tag{8}$$

and

$$D^{(2)}(b_\tau, \tau) = a_4(\tau) + a_5(\tau)[D^{(1)}(b_\tau, \tau)]^2. \tag{9}$$

Repeating the entire procedure for changing τ we can also estimate the dependence of the coefficients a_i on τ. Applying the algorithm, we have obtained the following results for the inertial range ($\tau \leq 5000$ seconds) $a_1 = -3.6\tau^{-0.08}, a_2 = 3.5\exp(-0.0001\tau), a_3 = -13.6\tau^{-0.2}, a_4 = 0.00035\tau^{0.7}, a_5 = 1.2\tau^{-0.3}$, and outside the inertial range ($\tau > 5000$ seconds) $a_1 = -0.5\tau^{0.16}, a_2 = 2, a_3 = -2.3, a_4 = 0.016\tau^{0.26}, a_5 = 1.75\tau^{-0.36}$. As an illustration, in Fig. 5 we show the dependence of the parameter a_4 on τ. One can notice a change in the dependence for $\tau \approx 5000$ seconds, i.e., at the end of inertial range.

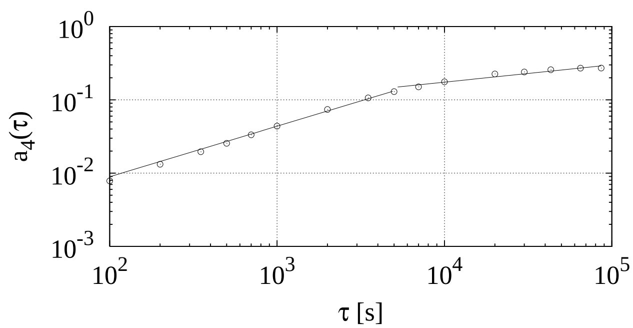

FIG. 5: Dependence of the parameter a_4 on scale τ (see Eq. (9)).

Parameterization of $D^{(1)}(b_\tau, \tau)$ and $D^{(2)}(b_\tau, \tau)$ (shown in Eqs. (8) and (9) correspondingly) with experimentally fitted parameters $a_i(\tau)$ allows us to solve numerically Eq. (6) with initial condition taken from parameterization of the experimental p.d.f. at a large scale τ_G, where the probability distribution of fluctuations is approximately Gaussian. Therefore we can compute numerically p.d.f. at scales $\tau < \tau_G$ and compare it to the experimental p.d.f., which allows us to verify directly our results. Such a comparison is shown in Fig. 6

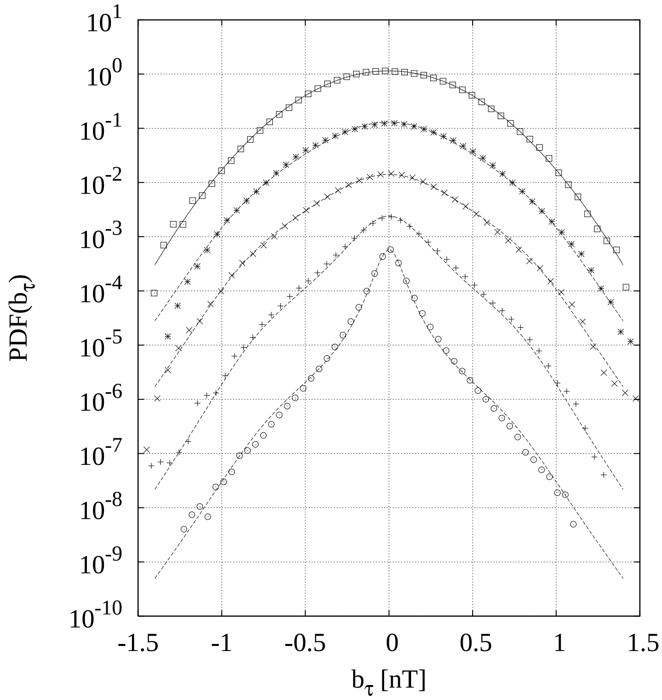

FIG. 6: Experimental probability distributions (points) and solution of the Fokker-Planck equation (dashed lines) for initial condition (solid line) obtained by approximation of the experimental p.d.f. by Gaussian distribution for $\tau = 86400$ seconds. We show the comparison of the experimental p.d.f. and solution of Eq. (6) for τ equal to 86400, 30000, 5000, 1000, 100 seconds (from the top). Probability distributions for different scales have been shifted in the vertical direction for clarity of presentation.

for $\tau_G = 86400$ seconds. As one can see there is a good agreement between experimental probability distributions and those computed from the Fokker-Planck equation.

V. DISCUSSION

We have shown that the Markov processes approach can be applied to the description of the turbulent cascade in fast solar wind turbulence. The Chapman-Kolmogorov equation is approximately satisfied in the inertial range, as well as for larger scales up to $\tau = 86400$ seconds. Numerical solution of the Fokker-Planck equation agrees well with experimental probability distributions obtained directly from data in the range of τ from 100 to 86400 seconds. Therefore, we can conclude that for intermittent solar wind turbulence, the Markov

processes approach can provide a mathematical formalism capable of explaining specific evolution of the shape of the probability distribution with scale changing from energy containing scale down to dissipation scale. Since the formalism describes properly evolution of the probability distribution with scale, obviously this should also work for structure functions, which are defined as appropriate moments of the probability distributions. Admittedly, direct analytical derivation of scaling properties of the structure functions can be difficult, but we expect that such studies can be done numerically.

Every Markov process must satisfy the Chapman-Kolmogorov equation (2), which express the condition that the probability density of transition from scale τ_2 to τ_1, can be subdivided into smaller steps, that is transition from scale τ_2 to τ', and then from scale τ' to τ_1. Therefore, in the case of a turbulent cascade, fulfillment of the Chapman-Kolmogorov equation can be interpreted as the presence of a local transfer mechanism in wave vector space. The question of locality of the energy transfer is of some interest, e.g., in the studies of dynamo mechanism to generate magnetic fields in astrophysical objects, where in helical MHD turbulence, nonlocal processes of generation of large-scale fields by small-scale helicities are studied in details (see, e.g., Sec. 6.2.1 of [11]). The question is also important for modeling MHD flows and numerical simulations, e.g., in large-eddy simulations, where low-pass filtering with respect to a cutoff wave number requires some assumptions concerning the transfer of energy around the cutoff wavenumber. Local and nonlocal transfer mechanisms can be distinguished in theoretical studies of turbulence via shell models or numerical simulations (see, e.g., [22, 23, 24]), but it is very difficult to study the property of turbulence using experimental data. The Markov processes approach seems to provide such a method. Namely, analyzing a time series from a turbulent flow we should be able to identify the character of the dominating transfer mechanism for a given quantity or between different quantities, i.e., we should be able to answer the question whether the mechanism is local or nonlocal.

Since our results suggest rather the Markovian character of the turbulent cascade in the solar wind, it indicates that the local transfer mechanism dominates in solar wind turbulence. Therefore dominating transfer of magnetic field fluctuations has similar character as in the case of Kolmogorov phenomenology describing turbulence in neutral fluids, where according to the picture of Richardson cascade, the energy transfer has local character in the wave vector space, i.e., the energy at a scale l is transfered mainly to comparable scales [10].

This result is somewhat surprising, because we analyze here magnetohydrodynamic turbulence, which is rather magnetic field dominated case. Therefore, according to the classical Iroshnikov-Kraichnan picture, due to the Alfvén effect, we should expect nonlocal influence of large-scale magnetic field on small-scale turbulent eddies, and so also nonlocal interactions between modes [11]. However, results of recent numerical simulations suggest that local transfer mechanisms are present in MHD turbulence [22, 23, 24]. Our paper provides experimental results confirming this observation for magnetic-to-magnetic field transfer.

Acknowledgments

This work has been supported by the Polish Ministry of Science and Higher Education through Grant No. N N202 4127 33.

---

[1] W. H. Matthaeus and M. L. Goldstein, J. Geophys. Res. **87**, 6011 (1982).

[2] M. L. Goldstein, D. A. Roberts, and W. H. Matthaeus, Annu. Rev. Astron. Astrophys. **33**, 283 (1995).

[3] C.-Y. Tu and E. Marsch, Space Sci. Rev. **73**, 1 (1995).

[4] M. L. Goldstein and D. A. Roberts, Phys. Plasmas **6**, 4154 (1999).

[5] E. Marsch and C. Y. Tu, Ann. Geophys. **12**, 1127 (1994).

[6] L. Sorriso-Valvo, V. Carbone, P. Veltri, G. Consolini, and R. Bruno, Geophys. Res. Lett. **26**, 1801 (1999).

[7] L. Sorriso-Valvo, V. Carbone, P. Giuliani, P. Veltri, R. Bruno, V. Antoni, and E. Martines, Planet. Space Sci. **49**, 1193 (2001).

[8] L. F. Burlaga, J. Geophys. Res. **106**, 15917 (2001).

[9] R. Bruno and V. Carbone, Living Reviews in Solar Physics **2**, 4 (2005).

[10] U. Frisch, *Turbulence. The legacy of A.N. Kolmogorov* (Cambridge: University Press, 1995).

[11] D. Biskamp, *Magnetohydrodynamic Turbulence* (Cambridge: University Press, 2003).

[12] G. Pedrizzetti and E. A. Novikov, J. Fluid Mech. **280**, 69 (1994).

[13] R. Friedrich and J. Peinke, Physica D **102**, 147 (1997).

[14] R. Friedrich and J. Peinke, Phys. Rev. Lett. **78**, 863 (1997).

[15] J. Davoudi and M. R. Tabar, Phys. Rev. Lett. **82**, 1680 (1999).

[16] R. Friedrich, J. Peinke, and C. Renner, Phys. Rev. Lett. **84**, 5224 (2000).

[17] C. Renner, J. Peinke, and R. Friedrich, J. Fluid Mech. **433**, 383 (2001).

[18] B. Hnat, S. C. Chapman, and G. Rowlands, Phys. Rev. E **67**, 056404 (2003).

[19] R. Schwenn, Space Sci. Rev. **124**, 51 (2006).

[20] A. Balogh, T. J. Beek, R. J. Forsyth, P. C. Hedgecock, R. J. Marquedant, E. Smith, D. J. Southwood, and B. T. Tsurutani, Astron. Astrophys. Suppl. Ser. **92**, 221 (1992).

[21] H. Risken, *The Fokker-Planck equation. Methods of solution and applications* (Springer Series in Synergetics, Berlin, New York: Springer, 2nd ed., 1989).

[22] O. Debliquy, M. K. Verma, and D. Carati, Phys. Plasmas **12**, 2309 (2005).

[23] A. Alexakis, P. D. Mininni, and A. Pouquet, Phys. Rev. E **72**, 046301 (2005).

[24] P. Mininni, A. Alexakis, and A. Pouquet, Phys. Rev. E **72**, 046302 (2005).